Arc Discharge Synthesis and Properties of Magnetic Nanoparticles

Sergey A. Novopasin, Marina A. Serebrjakova, Alexey V. Zaikovskii
Lab. of Rarefied Gases
Kutateladze Institute of Thermophysics
Novosibirsk, Russia
e-mail: sanov@itp.nsc.ru

Lubov G. Smolyaninova,
Sobolev Institute of Geology and Mineralogy
Novosibirsk, Russia
Tatiana U. Kardash
Boreskov Institute of Catalysis
Novosibirsk, Russia

***Abstract*—The composite Fe-C anode sputtering in a low pressure arc discharge has been used to produce Fe containing nanoparticles on a carbon matrix. The manufactured material was calcined stepwise in air from 300 to 1100 K. This procedure resulted in the formation of Fe oxides and oxidation of carbon and converting it into gas phase. The results show the change in morphology, chemical composition, crystalline phases and magnetic susceptibility properties with annealing temperature. This research is directed to elaborate on new technologies for producing magnetic nanoparticles and ferrofluids from their basis.**

Keywords – magnetic nanoparticles; arc dicharge; ferrofluids.

I. INTRODUCTION

The magnetic iron oxide nanoparticles are mainly used in ferrofluid technologies. Many chemical techniques are used to synthesize iron oxide nanoparticles for ferrofluids, including coprecipitation, hydrothermal reactions [1], sol–gel method [2], micro emulsions techniques [3], flow injection synthesis [4], aerosol/vapor methods, sonochemical reactions [5], electro spray synthesis [6], and electrochemical synthesis [7]. Nevertheless, the method mainly used for the generation of magnetite nanoparticles is chemical coprecipitation technique of iron salts [8] - [10]. Magnetic nanoparticles could not be kept as a powder because of their small size and strong interaction. Therefore, all the above mentioned technologies use surfactants to prevent agglomeration of magnetic nanoparticles directly in base fluids. In this paper, we present a new technology for manufacturing magnetic nanoparticles inside the carbon matrix, which allows the transportation of magnetic nanoparticles as a powder.

The details of experimental setup and used probing techniques are presented in section "Experimental Development". Section "Experimental Results" is devoted to the results obtained by Transmission Electron Microscopy (TEM), X-ray Diffraction (XRD), Thermo gravimetric analysis (TGA), Raman scattering (RS) and magnetic susceptibility measurements. It is underlined in conclusion section that the arc discharge technology is perspective for ferrofluid applications.

II. EXPERIMENTAL DEVELOPMENT

The experiments were carried out in a direct current electric arc, which had a current of 120 A, in the buffer gas (helium) at 25 Torr. The spray electrode (anode) was a graphite rod 70 mm in length and 7 mm in diameter. A hole (with the diameter of 4 mm) was drilled in the center of the electrode to be filled with graphite – carbonyl iron mixture powder. Fe/C weight ratio was 2/1. Monatomic spray products were diffused in the buffer gas from the hot zone of the arc, which resulted in cooling and heterogeneous condensation of the spray products. The composite material was precipitated on a cooled shield located at 5 cm from the arc discharge area. The synthesized material consist of iron containing nanoparticles on a carbon matrix. For the second step, the synthesized Fe-C composite was calcined for two hours in air at 200, 300, 400, 450, 500, 550, 600, 700 and 800 °C. This procedure resulted in the formation of Fe oxides and oxidation of carbon and removing it into the gas phase. TEM, XRD, TGA, RS and magnetic susceptibility measurements were used to test material properties at every step.

High-resolution TEM images were obtained using the JEM-2010 electron microscope (JEOL, Japan) with lattice-fringe resolution of 0.14 nm and accelerating voltage of 200 kV. The high-resolution images of periodic structures were analyzed by the Fourier method. Local energy-dispersive X-ray analysis (EDXA) was carried out using the EDX spectrometer (EDAX Co.), which was fitted with a Si (Li) detector, at (!!!) resolution of 130 eV. The samples for the HRTEM study were prepared on a perforated carbon film mounted on a copper grid.

XRD analysis was carried out using the Bruker D8Advance diffractometer, which was equipped with the Lynxeye (1D) linear detector, over the angular range of 10–75◦ at 2Θ = 0.05◦ with the storage time of 1 s for each point. Monochromatic CuK-radiation (1.5418˚A) was applied in these experiments.

TGA experiments were performed by the DTG60 H instrument (Shimadzu Scientific Instruments).

The Raman spectra were taken on the Spex Triplemate instrument (Princeton Instruments, USA) at the wavelength of 488 nm.

Magnetic susceptibility was measured by MS2 susceptibility/temperature system (Bartington, Great Britain).

III. EXPERIMENTAL RESULTS

A. Morphology of material

Electron microscopy of the synthesized material indicated that it consist of amorphous carbon particles with inclusions of crystal nanoparticles of 2–10 nm (see Figure 1). Calcinations in air resulted in carbon removal g, oxidation of

 ISBN: 978-1-61208-380-3

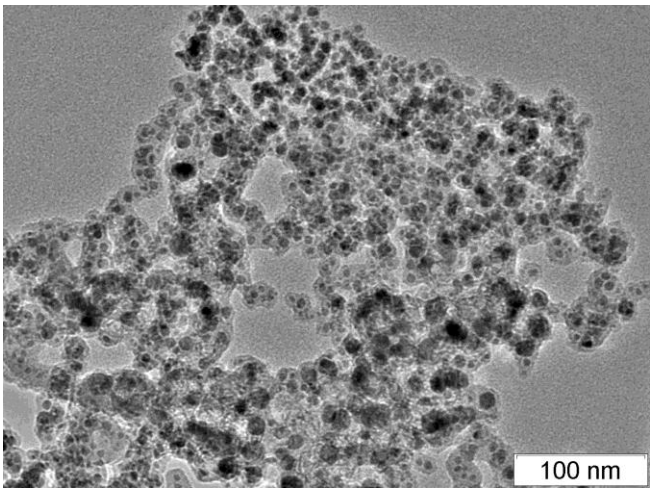

Figure 1. The morphology of synthesized material.

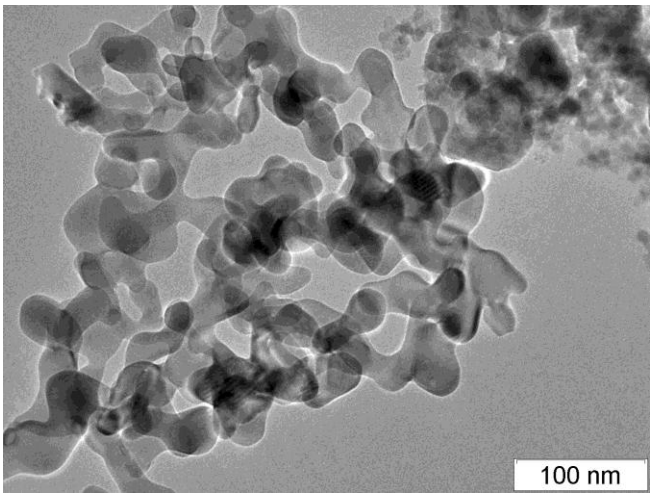

Figure 2. The morphology of the material calcined at 400 °C.

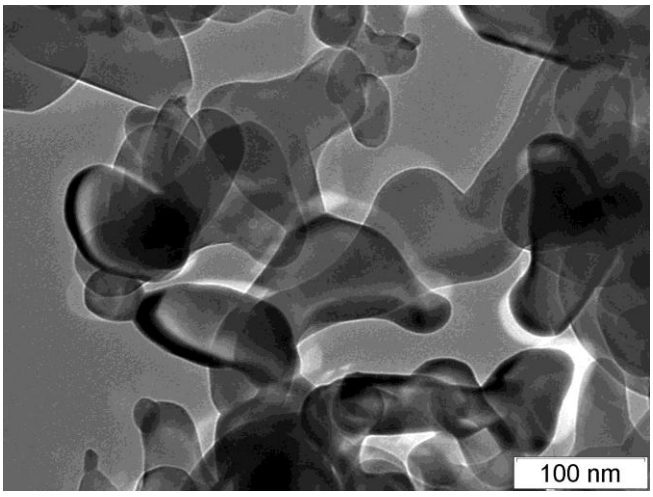

Figure 3. The morphology of the material calcined at 800 °C.

iron and junction of nanoparticles (see Figures 2, 3). The morphology was transformed from separate nanoparticles into the 3-D random connected structures with expending size and the temperature of calcinations increasing.

B. Thermogravimetric analysis

Thermogravimetric analysis of synthesized materials has been carried out in two ways. Firstly, is the use of DTG60 device, and secondly, is the step-wise calcinating at definite temperature for two hours and measuring the weight loss. Data are presented in Figure 4.

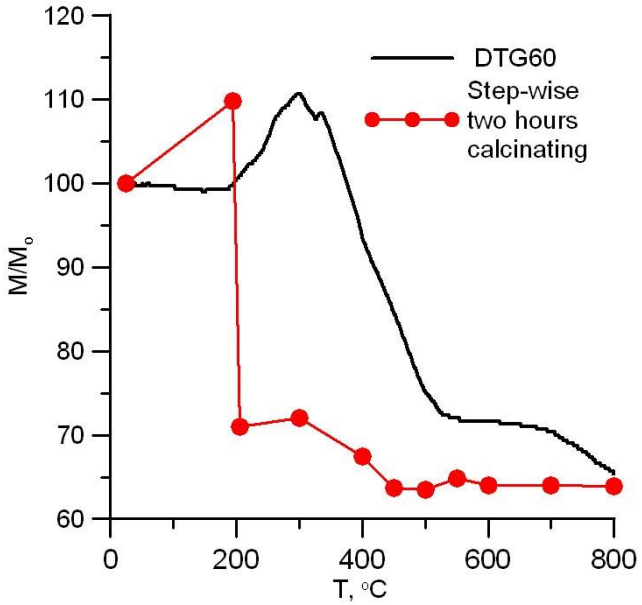

Figure 4. Thermogravimetric analysis.

Both curves show the weight increase at the initial stage. Obviously, it is due to oxidation of iron containing particles. The step-wise analysis demonstrates that at 200 °C, most part of carbon reacts with oxygen (Fe nanoparticles probably served as catalyst) and it is removes from the sample. The reason for the observed difference is the fact that the reaction times in both cases differed considerably.

C. Phase composition

X-ray diffraction spectroscopy shows that the synthesized material consists of graphite, iron and iron carbide (see Figure 5). Calcination of this material results in a change in composition. Even when calcinating at 300 °C, both α-Fe_2O_3 and γ-Fe_2O_3 crystalline forms of iron oxide appeared, but iron and iron carbide lines disappeared in the spectrum (see Figure 6).

X-ray diffraction spectroscopy shows that the synthesized material consists of graphite, iron and iron carbide (see Figure 5). Calcination of this material results in

 ISBN: 978-1-61208-380-3

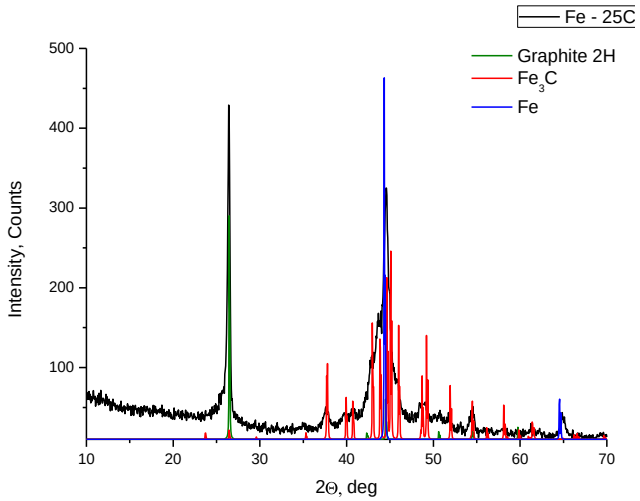

Figure 5. XRD spectrum of synthesized material.

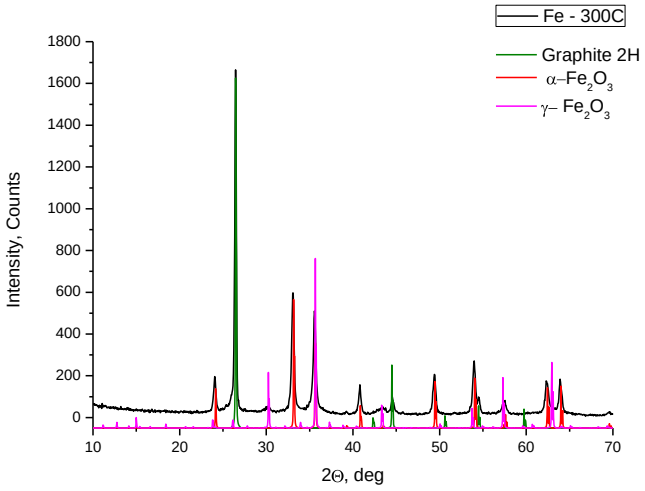

Figure 6. The XRD spectrum of material calcinated at 300 °C.

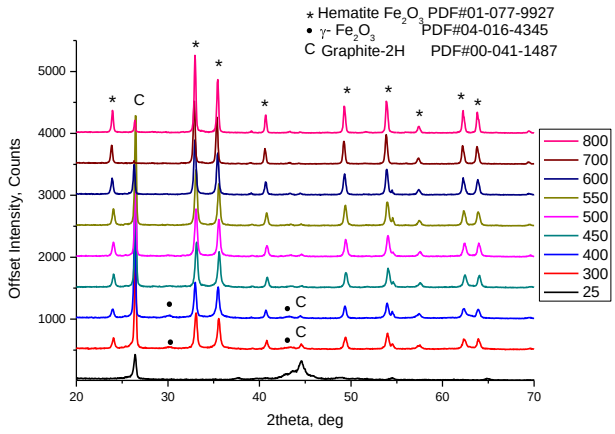

Figure 7. The XRD spectra of material calcinated at different temperatures..

change in composition. Even when calcinating at 300 °C, both α-Fe_2O_3 and γ-Fe_2O_3 crystalline forms of iron oxide appeared, but iron and iron carbide lines disappeared in the spectrum (see Figure 6).

Further calcinations resulted in γ-Fe_2O_3 disappearing and growing intensity of α-Fe_2O_3 (non-magnetic) as shown in Figure 7. It is interesting to note that graphite line does not disappear even at 800 °C.

D. Raman spectroscopy

Raman spectra of materials calcinated at different temperatures are shown in Figure 8. Practically, no signals of iron oxides are seen up to the calcination temperature of 300 °C. The main lines are: 225, 299, 400, 500, and 613 cm^{-1}. Most lines identify α-Fe_2O_3, but line 500 cm^{-1} is the sum of γ-Fe_2O_3 (strong intensity) and α-Fe_2O_3 (week intensity) [11]. Data obtained by RS confirm XRD data, but we suppose that for our materials, XRD analysis is preferable for identification of phase composition with respect to Raman scattering.

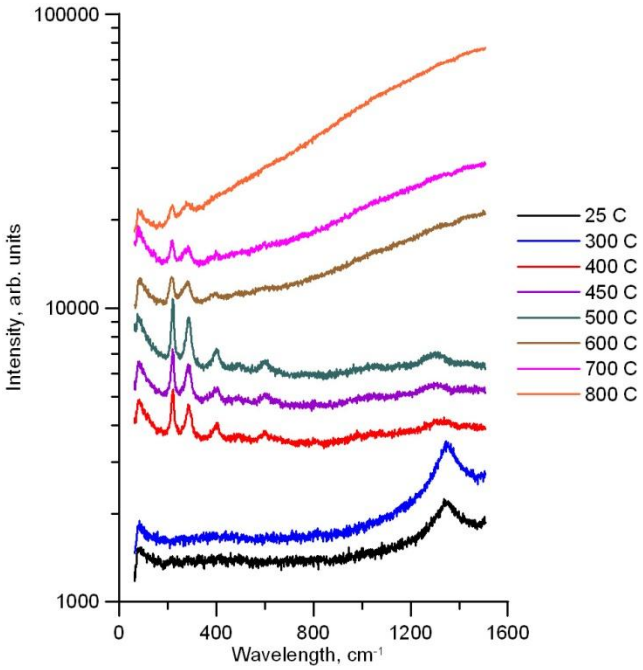

Figure 8. Raman spectrum of material calcinated at different temperatures.

E. Magnetic susceptibility

To measure magnetic susceptibility, about 200 mg of synthesized material was loaded into the measuring dish. The temperature dependency was measured by heating the sample and then cooling it in air. Results are shown in Figure 9. Heating in air resulted in chemical reaction with oxygen and phase transition as it was noted before. So, the final weight of the sample was about 135 mg in accordance with TGA measurements (see Figure 4). The same reason is that magnetic susceptibility was close to zero, while cooling.

 ISBN: 978-1-61208-380-3

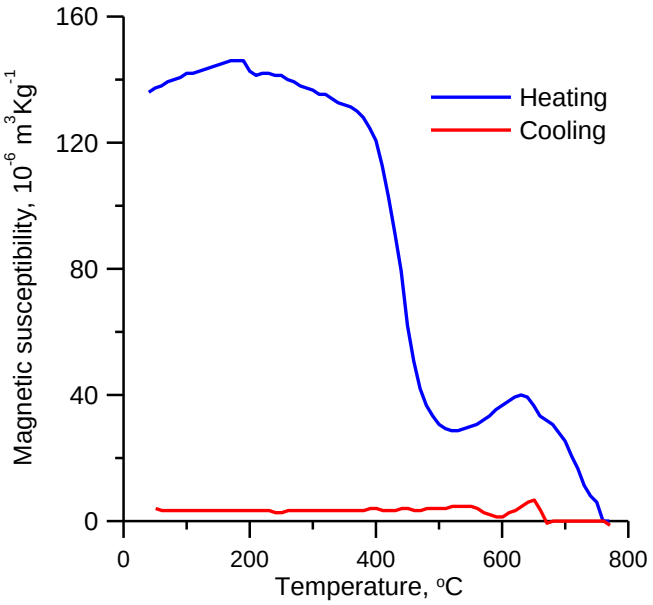

Figure 9. Magnetic susceptibility vs. temperature.

IV. CONCLUSIONS

The arc discharge technology of manufacturing magnetic nanoparticles has been suggested and realized. The morphology, phase composition and magnetic susceptibility have been measured at calcination in air of up to 800 °C. We consider the synthesized material perspective for ferrofluid applications.

The future research of this work is directed to optimization of the arc discharge parameters to reach the maximal value of magnetic susceptibility.

ACKNOWLEDGMENT

This research was funded by Russian Ministry of Education and Science. Project Identifier: RFMEFI60414X0004.

REFERENCES

[1] J. Wan, et al., "A soft-template-assisted hydrothermal approach to single crystal Fe3O4 nanorods", J. Cryst. Growth, vol. 276, no. 3, 2005, pp. 571–576.

[2] C. Albornoz and S. E. Jacobo, "Preparation of a biocompatible magnetic film from an aqueous ferrofluid", J.Magn.Magn.Mater. vol. 305, no.1, 2006, pp. 12–15.

[3] A. B. Chin and I. I. Yaacob, "Synthesis and characterization of magnetic iron oxide nanoparticles via w/o microemulsion and Massart's procedure", J.Mater. Process.Technol., vol. 191, no. 1, 2007, pp. 235–237.

[4] G. Salazar-Alvarez, M.Muhammed, and A. A. Zagorodni, "Novel flow injection synthesis of iron oxide nanoparticles with narrow size distribution", Chem. Eng. Sci., vol. 61, no. 14, 2006, pp. 4625–4633.

[5] E. H. Kim, Y. Ahn, and H. S. Lee, "Biomedical applications of super paramagnetic iron oxide nanoparticles encapsulated within chitosan", J. Alloys Compd., vol. 434, 2007, pp. 633–636.

[6] S. Basak, D.-R. Chen, and P. Biswas, "Electro spray of ionic precursor solutions to synthesize iron oxide nanoparticles: modified scaling law", Chem. Eng. Sci., vol. 62, no. 4, 2007, pp. 1263–1268.

[7] D. Ramimoghadam, S. Bagheri, and S. Bee Abd Hamid, "Progress in electrochemical synthesis of magnetic iron oxide nanoparticles", Journal of Magnetism and Magnetic Materials, vol. 368, 2014, pp. 207–229.

[8] S. A. Morrison, et al., "Magnetic and structural properties of nickel zinc ferrite nanoparticles synthesized at room temperature", J.Appl.Phys., vol. 95, no. 11, 2004, pp. 6392–6395.

[9] J. Qiu, et al., "Preparation and characterization of porous ultrafine Fe_2O_3 particles", Mater.Res.Bull., vol. 40, no. 11, 2005, pp. 1968–1975.

[10] S.-J. Lee, et al., "Magnetic enhancement of iron oxide nanoparticles encapsulated with poly(D,L-latide-co-glycolide)", Colloids Surf.,A, vol. 255, no. 1, 2005, pp. 19–25.

[11] D. L. A. de Faria, S. Venancio Silva, and M. T. de Oliveira, "Raman microspectroscopy of some iron oxides and oxyhydroxides", J. Raman Spectrosc. vol. 28, 1997, pp. 873–878.

 ISBN: 978-1-61208-380-3